do not reach the Hartree–Fock limit at the DZ quality of basis sets. Second, from the UPS results discussed above, the first IP of the porphyrins appears to be about 0.6–1.0 eV more than the computed Koopmans' IP, even at the Hartree–Fock limit. Third, many of the electron-deficient porphyrins currently known are sterically hindered dodecasubstituted porphyrins, which, on the basis of available crystallographic data,[6g,48] are probably highly buckled. In this survey of substituent effects, we have not studied any buckled porphyrins. From this point of view, fluoro and cyano substituents are among the least sterically demanding among electronegative substituents and, therefore, are the least likely to cause buckling. Fourth, there may be unexpectedly large relaxation energies associated with ionizations of certain substituted porphyrins. Some of these questions are currently being pursued in our laboratory.

V. Conclusions

XPS and all-electron ab initio SCF calculations have shown the 1s energies of the central nitrogens to be sensitive probes of the electronic effects of peripheral substituents in porphyrins. Estimates of substituent effects on the highest occupied π MOs have also been obtained. The results of our calculations have been found to be in generally good agreement with experiment. The present study shows that very large substituent effects are possible with suitable arrays of electronegative substituents. Effects of this magnitude should be responsible for a wide range of physical and chemical properties among the porphyrins.

Acknowledgment. This research was supported by the National Science Foundation (grants to P.G.G. and J.A.), grants of computer time from the Minnesota Supercomputer Institute, Minneapolis, and from the National Center for Supercomputing Applications, Urbana–Champaign, a Graduate School Dissertation Fellowship from the University of Minnesota (to A.G.), and XPS facilities at the Regional Instrumentation Center for Surface Analysis at the University of Minnesota and at the Perkin-Elmer Physical Electronics Division Laboratory at Eden Prairie, MN.

---

(48) (a) Barkigia, K. M.; Chantranupong, L.; Smith, K. M.; Fajer, J. *J. Am. Chem. Soc.* **1988**, *110*, 7566. (b) Barkigia, K. M.; Berber, M. D.; Fajer, J.; Medforth, C. J.; Renner, M. W.; Smith, K. M. *J. Am. Chem. Soc.* **1990**, *112*, 8851.

Unimolecular Chemistry of Protonated Ethyl Cyanide and Ethyl Isocyanide: An Experimental and Molecular Orbital Study

Guy Bouchoux,*[†] Minh Tho Nguyen,[‡] and Pierre Longevialle[§]

Contribution from the Department of Chemistry, DCMR Ecole Polytechnique, F-91128 Palaiseau Cedex, France, Department of Chemistry, University of Leuven, B-3001-Leuven, Belgium, and Institut de Chimie des Substances Naturelles du CNRS, F-91190-Gif sur Yvette Cedex, France.

Received March 30, 1992

Abstract: The unimolecular reactivity of both protonated forms of ethyl cyanide (**1**) and ethyl isocyanide (**2**) in the gas phase has been examined experimentally using deuterium labeling and mass analyzed ion kinetic energy spectrometry. It has been shown that both species isomerize into weak π-complexes between ethene and $HCNH^+$ (**3** and **4**), which may further dissociate or interconvert either by reorientation or by cycloaddition–cycloreversion. Relevant portions of the $C_3H_6N^+$ potential energy surface have been explored using ab initio molecular orbital calculations up to the MP2/6-311++G**//MP2/6-31G** + ZPE level. These data provide new examples of the 1,2 elimination processes which require the intermediacy of loosely bound ion–neutral complexes. This study is also of interest in interstellar and planetary atmosphere chemistry, particularly in view of the possible formation of ethyl isocyanide along with ethyl cyanide by dissociative recombination of both protonated forms **2** or **1**, respectively.

Introduction

The gas-phase chemistry of cyanides and isocyanides is of interest not only in fundamental organic chemistry but also in interstellar[1] and planetary high atmosphere[2] chemistry where it is generally agreed that they derive from dissociative recombination of their protonated counterparts[3]

$$MH^+ + e \rightarrow M + H^\cdot$$

$$(M = RCN \text{ or } RNC)$$

While a number of studies have been devoted to the protonated forms of HCN, HNC, CH_3CN, CH_3NC, n-C_3H_7CN, and i-C_3H_7CN,[4-20] the protonated ethyl cyanide and ethyl isocyanide have received less attention,[14,15,18,19,20] and, to date, no detailed examination of their unimolecular reactivity has been reported even though ethyl cyanide is among the 80 or so species yet identified in the interstellar media.[1]

This article presents the results of an experimental and theoretical investigation on the isomerisation and dissociation of

---

[†] Ecole Polytechnique.

[‡] University of Leuven.

[§] Institut de Chimie des Substances Naturelles.

(1) (a) Duley, W. W.; Williams, D. A. *Interstellar Chemistry* Academic Press: New York, 1984. (b) Turner, B. E. *Space Sci. Rev.* **1989**, *51*, 235.

(2) (a) Shlager, H.; Arnold, F. *Planet Space Sci.* **1985**, *33*, 1363. (b) Arijs, E.; Brasseur, G. *J. Geophys. Res.* **1986**, *91*, 4003.

(3) For a discussion on this problem see: (a) Millar, T. J.; DeFrees, D. J.; McLean, A. D.; Herbst, E. *Astron. Astrophys.* **1988**, *194*, 250. (b) Herbst, E.; Leung, C. M. *Astron. Astrophys.* **1990**, 233, 177, and ref 1.

(4) Burgers, P. C.; Terlouw, J. K.; Weiske, T.; Schwarz, H. *Chem. Phys. Lett.* **1986**, *132*, 69, and references therein.

(5) Nguyen, M. T.; Ha, T. K. *J. Chem. Soc., Perkin Trans. 2* **1984**, 1401.

(6) Wurthwein, E. U. *J. Org. Chem.* **1984**, *49*, 2971.

(7) DeFrees, D. J.; McLean, A. D.; Herbst, E. *Astrophys. J.* **1985**, *293*, 236.

(8) Kemper, P. R.; Bass, L. M.; Bowers, M. T. *J. Phys. Chem.* **1985**, *89*, 1105.

(9) Knight, J. S.; Freeman, C. G.; McEwan, M. J. *J. Am. Chem. Soc.* **1986**, *108*, 1404.

(10) Wincel, H.; Wlodek, S.; Bohme, D. K. *Int. J. Mass Spectrom. Ion Proc.* **1988**, *84*, 69.

(11) Wincel, H.; Fokkens, R. H.; Nibbering, N. M. M. *Int. J. Mass Spectrom. Ion Proc.* **1989**, *88*, 241.

(12) Meot Ner, M.; Karpas, Z. *J. Phys. Chem.* **1986**, *90*, 2206.

Table I. Mass Analyzed Ion Kinetic Energy Spectra of $C_3H_6N^+$ Metastable Ions (Ion Relative Abundances)[a]

		m/z				
		32	31	30	29	28
1	$C_2H_5CNH^+$				7	93
1a	$C_2H_5CND^+$			4	70	26
1b	$CH_3CD_2CNH^+$		5	2	20	73
1c	$CH_3CD_2CND^+$	3	4	8	74	11
1d	$CD_3CH_2CNH^+$	(4)	(3)	12	69	12
1e	$CD_3CH_2CND^+$	(5)		63	30	2
2	$C_2H_5NCH^+$				8	92
2a	$C_2H_5NCD^+$			1	95	4

[a] Values in parentheses are only indicative; artifact peaks were present at these *m/z* values in the experimental conditions used.

$C_2H_5CNH^+$ (**1**) and $C_2H_5NCH^+$ (**2**) ions in the gas phase. Mass spectrometry in conjunction with deuterium labeling has provided experimental information on the dissociation of ions **1** and **2** of low internal energy. Interpretation of the data is supported by thermochemistry as well as detailed molecular orbital calculations of the relevant parts of the $C_3H_6N^+$ potential energy surface.

Experimental and Computational Details

The experiments were carried out with a VG-ZAB-2F double focusing mass spectrometer (B–E) operating in the chemical ionization mode. The accelerating voltage was set at 8 kV, the electron energy at 150 eV, and the emission current at 0.5 mA. The source temperature was 180 °C. The mass analyzed ion kinetic energy (MIKE) spectra of metastable ions were obtained, as usual, by selecting with the magnet the ion to be studied and scanning the electrostatic analyzer voltage. Methane and deuteromethane were used as reagent gases in the chemical ionization experiments.

CH_3CD_2CN was prepared by refluxing propionitrile during 6 h in a mixture of MeOD, MeONa, and D_2O.[30] After extraction with dichloromethane, the product was purified by distillation. CD_3CH_2CN was prepared by the method described by Lohaus[21] from a commercial sample of CD_3CH_2COOH and purified by gas chromatography.

Ab initio molecular orbital calculations were carried out using the Monstergauss[22] and Gaussian 90[23] suites of programs. Structures of the stationary points considered were initially optimized at the Hartree–Fock (HF) level with the d-polarization 6-31G* basis set and characterized by harmonic vibrational wavenumbers computed at this HF/6-31G* level making use of analytical force constants. The structures were then reoptimized at the second-order Moller–Plesset perturbation theory (MP2) level with the dp-polarization 6-31G** basis set. Improved relative energies were finally estimated from MP2 calculations using the sp-diffuse plus dp-polarization 6-311++G** basis set[23] and MP2/6-31G** optimized geometries. The zero-point energy corrections (ZPE) were estimated from vibrational wavenumbers at the HF/6-31G* level.

Throughout this paper, bond lengths are given in angstroms, bond angles in degrees, total energies in hartrees, and zero-point and relative energies in kJ mol^{-1}. Unless otherwise noted, relative energies in the text refer to the MP2(F)/6-311++G**//MP2/6-31G** + ZPE level of theory.

Results and Discussion

Experiment. Unimolecular decomposition of both metastable ions $C_2H_5CNH^+$ (**1**) and $C_2H_5NCH^+$ (**2**) leads essentially to protonated hydrogen cyanide following ethene elimination (Table I). In the same *m/z* region, a small signal (7% and 8% for **1** and **2**, respectively) appears corresponding to the formation of $C_2H_5^+$ by loss of a (H, C, N) neutral. Analysis of the metastable peak profile corresponding to the dissociations $1 \rightarrow HCNH^+ + C_2H_4$ and $2 \rightarrow HCNH^+ + C_2H_4$ reveals two different situations. In the case of **1**, the peak is simple Gaussian and broad ($T_{0.5}$ = 58 meV and T_{av} = 160 meV). In contrast, the metastable peak in the case of **2** is narrow ($T_{0.5}$ = 4–7 meV) (in both cases, $T_{0.5}$ values have been corrected for the main beam width[24]). Furthermore, both collisionally induced dissociation spectra of **1** and **2** are clearly distinct and allow a facile differentiation of both ion structures.[14] These data indicate that (i) isomerization $1 \rightarrow 2$ is not an easy process; (ii) dissociation $2 \rightarrow HCNH^+ + C_2H_4$ probably occurs at its thermochemical threshold, and (iii) dissociation $1 \rightarrow HCNH^+ + C_2H_4$ is preceded by a rate-determining isomerization step.

Chart I

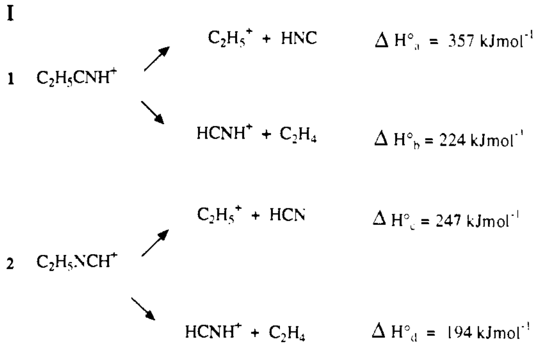

Scheme I

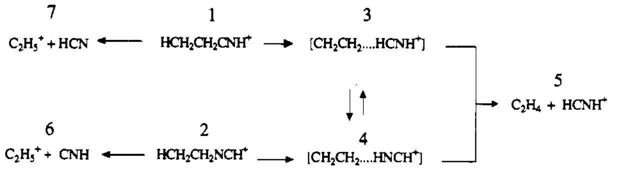

D-labeling experiments provide further information concerning decomposition of **1** and **2**. For protonated ethyl isocyanide (**2**) it is evident from Table I that the deuteron in $C_2H_5NCD^+$ (**2a**) retains almost entirely (96%) its individuality during ethene elimination. Similarly, ethyl cation is mostly (>88%) formed without H-exchange. By contrast, the MIKE spectrum of $C_2H_5CND^+$ (**1a**) shows a significant (ca. 28%) proportion of C_2H_3D in the ethene elimination revealing the occurrence of exchanges of the D atom with the hydrogens of the saturated aliphatic chain. Protonated ethyl-*2,2-d*$_2$ cyanide (**1b**) loses preferentially CH_2CD_2 but 22% CH_2CHD elimination shows the participation of H–D exchanges involving the position C(2). These observations are confirmed by the spectrum of $CH_3CD_2CND^+$ (**1c**) whose major signal corresponds to (C, N, H, D)$^+$ ions, i.e., an apparently specific 1,2 elimination, along with 20% of d_1- and d_3-labeled ethene elimination. A parallel situation is observed for the complementary parent ion $CD_3CH_2CNH^+$ (**1d**); the nonspecific elimination of d_1- and d_3-labeled ethene amounts in this case to 26%. Finally, for $CD_3CH_2CND^+$ (**1e**) the latter process leads essentially to ethene-d_3 elimination (31%).

These experimental results may be interpreted in terms of a simple model describing ethene elimination as occurring by two distinct processes: (A) specific β-elimination without H-exchange or (B) elimination after the statistic randomization of all six H atoms. It is clear from Table II that neither model A nor B alone may explain the results. If x and $(1 - x)$ represent the complementary participations of A and B in the process and i the possible isotope effect on H transfers, a couple of equations may be derived from each compound from the data in Table II. The solutions for x and i are reasonably concordant and indicate a participation of A and B in the mean ratio 60/40 and no isotope effect (model C in Table II).

---

(13) McEwan, M. J.; Denison, A. B.; Huntress, W. T., Jr.; Anicich, V. G.; Snodgrass, J.; Bowers, M. T. *J. Phys. Chem.* **1989**, *93*, 4064.

(14) Bouchoux, G.; Flament, J. P.; Hoppilliard, Y.; Tortajada, J.; Flammang, R.; Maquestiau, A. *J. Am. Chem. Soc.* **1989**, *111*, 5560.

(15) Wincel, H.; Fokkens, R. H.; Nibbering, N. M. M. *Int. J. Mass Spectrom. Ion Proc.* **1989**, *91*, 339.

(16) Deakyne, C. A.; Meot Ner, M. *J. Phys. Chem.* **1990**, *94*, 232.

(17) Wincel, H.; Fokkens, R. H.; Nibbering, N. M. M. *J. Am. Soc. Mass Spectrom.* **1991**, *2*, 178.

(18) Aue, D. H.; Webb, H. M.; Bowers, M. T. *J. Am. Chem. Soc.* **1975**, *97*, 4137.

(19) Meot Ner, M.; Karpas, Z.; Deakyne, C. A. *J. Am. Chem. Soc.* **1986**, *108*, 3913.

(20) Marriott, S.; Topsom, R. D.; Lebrilla, C. B.; Koppel, I.; Mishima, M.; Taft, R. W. *J. Mol. Struct.* (*THEOCHEM*) **1986**, *137*, 133.

(21) Lohaus, G. *Org. Syn.* **1970**, *50*, 18.

(22) Peterson, M. R.; Poirier, R. A. Program MONSTERGAUSS 80, University of Toronto, Ontario, Canada.

(23) Program GAUSSIAN 90, Gaussian Inc., Pittsburgh, PA, 1991.

(24) Holmes, J. L.; Osborne, A. D. *Int. J. Mass Spectrom. Ion. Phys.* **1977**, *23*, 189.

Table II. Probability of $XCNX^+$ (X = H or D) Ion Formation Assuming (A) Specific β-Elimination, (B) Ethene Elimination after Complete H–D Randomization, (C) a Mixture of Mechanisms A (60%) and B (40%), Compared with Experiment (Exp)

$C_3X_6N^+$ precursor		$DCND^+$	$HCND^+$	$HCNH^+$
$C_2H_5CND^+$ (**1a**)	A		100	
	B		33	67
	C		73	27
	exp		73	27
$CH_3CD_2CNH^+$ (**1b**)	A			100
	B	7	53	40
	C	3	21	76
	exp	2	21	77
$CH_3CD_2CND^+$ (**1c**)	A		100	
	B	20	60	20
	C	8	84	8
	exp	9	80	11
$CD_3CH_2CNH^+$ (**1d**)	A		100	
	B	20	60	20
	C	8	84	8
	exp	13	74	13
$CD_3CH_2CND^+$ (**1e**)	A	100		
	B	40	53	7
	C	76	21	3
	exp	66	32	2

Scheme II

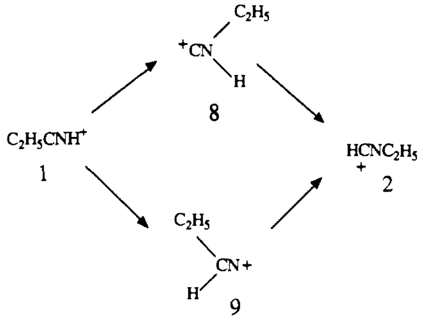

The same approach cannot be applied to the loss of (C, N, H) because of the poor intensity of the relevant peak in the spectrum. Nevertheless, it may be observed that (m/z 28)/(m/z 29) abundance ratios are similar in the spectra of **1** and **2**. This is somewhat surprising with regard to the corresponding thermochemistry. If it is assumed that **1** expels HNC and **2** expels HCN to produce $C_2H_5^+$, the reaction enthalpies may be calculated from tabulated ΔH_f° [25] and are shown on Chart I. While it seems possible to detect both ions m/z 28 and m/z 29 from metastable ions **2** due to the reasonably small difference $\Delta H_c^\circ - \Delta H_d^\circ = 53$ kJ mol^{-1}, the same abundance ratio from metastable **1** seems hard to reconcile with the difference $\Delta H_a^\circ - \Delta H_b^\circ = 133$ kJ mol^{-1}.

Molecular Orbital Calculations. The mechanistic model proposed to account for the observations mentioned above is based on previous results established in other β-elimination processes of protonated alcohols[26,27] or amines[28] in the gas phase. It is a stepwise process with an intermediate proton bound complex (Scheme I). Note that the rotation of the $HCNH^+$ moiety within the complexes **3** ⇌ **4** opens up a possible pathway for the interconversion **1** ⇌ **2**.

In order to investigate further the unimolecular chemistry of protonated ethyl cyanide (**1**) and protonated ethyl isocyanide (**2**), several additional isomerization pathways have also been examined. Those shown in Scheme II are all relevant to potential reactions assumed to occur for lower homologues $HCNH^+$, CH_3CNH^+, and CH_3NCH^+ in interstellar media. Their investigation presents therefore an additional interest in this regard.

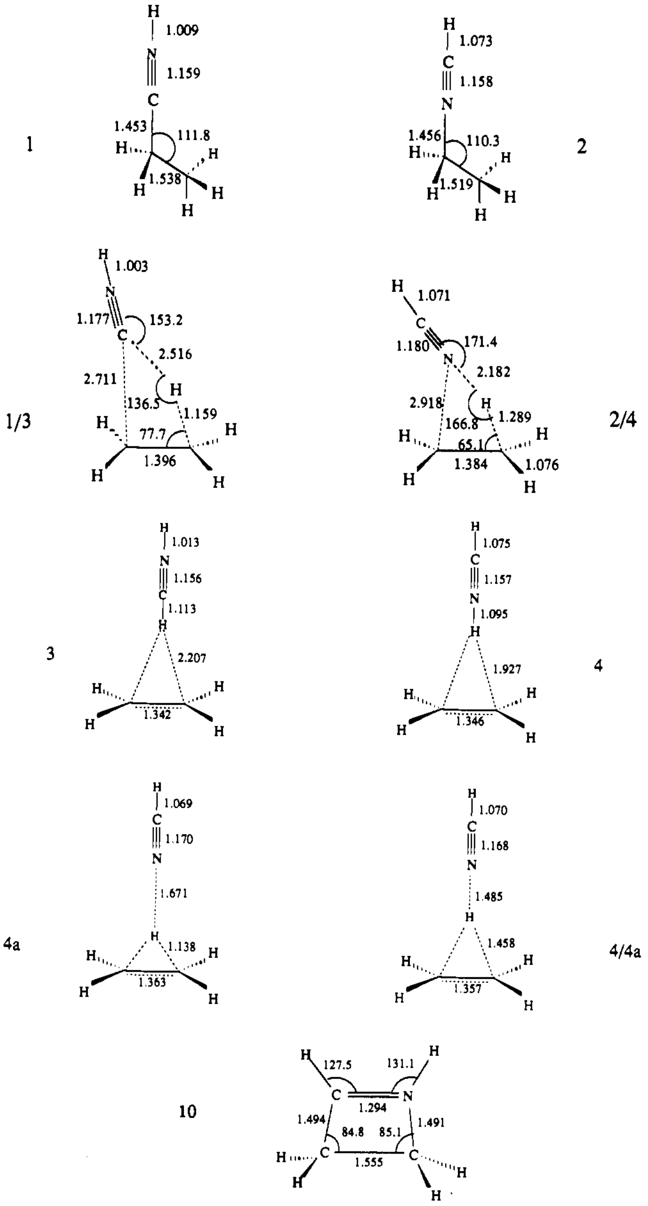

Figure 1. Selected geometrical parameters (at MP2/6-31G**) of minima and transition structures associated with β-elimination of protonated ethyl cyanide (**1**) and ethyl isocyanide (**2**).

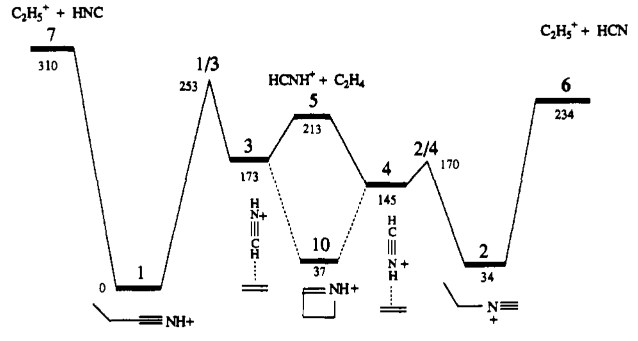

Figure 2. Calculated potential energy profile (at MP2(F)/6-311++G** + ZPE using MP2/6-31G**-geometries) for isomerization and dissociation of $C_2H_5CNH^+$ (**1**) and $C_2H_5NCH^+$ (**2**). Energy values are given in kJ mol^{-1}.

(a) β-Elimination via Ion–Neutral Complexes. The interconversions depicted in Scheme I have been examined using MO calculations. Geometrical parameters optimized at the MP2/6-31G** level for the equilibrium structures **1–7** and **10** and

---

(25) Lias, S. G.; Bartmess, J. E.; Liebman, J. F.; Holmes, J. L.; Levin, R. D.; Mallard, W. G. Gas Phase Ion and Neutral Thermochemistry. *J. Phys. Chem. Ref. Data* **1988**, *17*, Suppl. No. 1.

(26) Bouchoux, G.; Hoppilliard, Y. *J. Am. Chem. Soc.* **1990**, *112*, 9110.

(27) Swanton, D. J.; Marsden, D. C. J.; Radom, L. *Org. Mass Spectrom.* **1991**, *26*, 227.

(28) Reiner, E. J.; Poirier, R. A.; Peterson, M. R.; Csizmadia, I. G.; Harrison, A. G. *Can. J. Chem.* **1986**, *64*, 1652.

Table III. Total, Zero-Point, and Relative Energies for $C_3H_6N^+$ Ion Structures

		MP2(F) – total energies^b			relatives energies		
structure^a	symmetry	6-31G**	6-311++G**	ZPE^c	MP2/ 6-31G**	MP2/ 6-311++G**	MP2+ZPE^d
$C_2H_5CNH^+$ **1**	C_s	−171.874 88	−171.989 40	241	0	0	0
$C_2H_5NCH^+$ **2**	C_s	−171.863 84	−171.977 03	242	29	33	34
$C_2H_4 \cdots HCNH^+$ **3**	C_{2v}	−171.804 34	−171.916 69	229	185	183	173
$C_2H_4 \cdots HNCH^+$ **4**	C_{2v}	−171.813 91	−171.930 03	229	160	156	145
$C_2H_5^+ \cdots NCH$ **4a**	C_{2v}	−171.809 42	−171.924 89	219	172	169	150
TS **1/3**	C_s	−171.769 33	−171.885 51	219 (411i)	277	273	253
TS **2/4**	C_s	−171.802 77	−171.917 56	220 (289i)	189	189	170
TS **4/4a**	C_{2v}	−171.809 26	−171.925 02	215 (1541i)	172	169	146
ring 10	C_s	−171.867 53	−171.979 53	253	19	26	37
$HCNH^+ + C_2H_4$ **5**		−171.784 53	−171.902 67	224	237	228	213
$HCN + C_2H_5^+$ 6		−171.775 55	−171.892 06	217	261	256	234
$HNC + C_2H_5^+$ 7		−171.743 51	−171.862 37	214	345	334	310

[a] Based on MP2/6-31G** geometries given in Figure 1. [b] Using full set of MO's. [c] At the HF/6-31G* level In parentheses are the imaginary wavenumbers in cm^{-1}. [d] Including MP2/6-311++G** relative energies and ZPE's. The latter are scaled by 0.89 to account for systematic overestimation.

Table IV. Total, Zero-Point, and Relative Energies of Stationary Points Related to the **1**–**2** Isomerization

		total energies			relatives energies		
structure^a	symmetry	HF/6-31G*	MP2(F)/6-311++G**^{b}	ZPE^c	HF	MP2	MP2 + ZPE^d
$C_2H_5CNH^+$ **1**	C_s	−171.277 01	−171.986 75	241	0	0	0
$C_2H_5NCH^+$ **2**	C_s	−171.265 14	−171.973 74	242	31	34	35
$C_2H_5(H)N{=}C^+$ **8**	C_1	−171.192 47	−171.878 32	236	222	285	280
TS **1/8**	C_1	−171.178 41	−171.863 60	222 (123i)	259	323	307
TS **2/8**	C_1	−171.145 20	−171.813 28	223 (1411i)	346	455	439
TS **1/2**	C_1	−171.164 10	−171.852 64	228 (195i)	296	354	342

[a] Based on HF/6-31G* geometries. [b] Using full sets of MO's. [c] At the HF/6-31G*. In parentheses are the imaginary wavenumbers in cm^{-1}. [d] Including MP2/6-311++G** relative energies and ZPE's. The latter are scaled by 0.89.

transition structures **1/3**, **2/4**, and **4/4a** are given in Figure 1. Relevant total and relative energies are summarized in Table III. A schematic potential energy profile is displayed in Figure 2.

The first point which deserves comment concerns the structure of the $(C, N, H_2)^+$ product. It seems now established that among the three structures $HCNH^+$, CNH_2^+, and H_2CN^+, the most stable is the linear $HCNH^+$ ($\Delta H_f° = 947$ kJ mol^{-1} [25]). Next is H_2NC^+ ($\Delta H_f° = 1109 \pm 38$ kJ mol^{-1} [25]). The third isomer H_2CN^+ seems to be a saddle point in its singlet state but is a stable minimum on the triplet potential energy surface; these two structures lie ca. 300 and 500 kJ mol^{-1} above $HCNH^+$ respectively.[29] Clearly, $HCNH^+$ is the only possible structure for m/z 28 fragment ions from metastable **1** and **2** ions.

Formation of $HCNH^+$ from **1** and **2** was found to proceed by C–C or C–N bond lengthening accompanied by a displacement of the HNC or HCN group toward the methyl group. This motion is accompanied by slight C–H bond elongation and CCH bond angle closure inside the ethyl moiety. These geometrical modifications are the main components of the imaginary vibrational mode which characterize transition structures **1/3** and **2/4** (Figure 1). The C- - -H or N- - -N distances remain rather long in both TS's and that is similar to the transition structure previously found for the $C_2H_5OH_2^+$ ion.[26,27]

A slight reorganization involving mainly "internal protonation" of HNC or HCN gives rise to ion–neutral complexes **3** or **4**. These structures are clearly proton bound associations in which one of the hydrogens of $HCNH^+$ interacts with the π electrons of the ethene molecule. The binding energies of these complexes are equal to ca. 41 and 68 kJ mol^{-1} for **3** and **4** respectively. While a weak complex between ethyl cation and HNC cannot be found, the complex **4a** between ethyl cation and HCN has been located at the MP2/6-31G** level. In addition, a transition structure connecting both complexes **4** and **4a** has also been found (cf. Figure 1). Nevertheless, this transition structure TS **4/4a** which lies marginally above the complex **4a** at the MP2/6-31G** level (0.5 kJ mol^{-1}) turns out to lie below **4a** at the higher MP2/6-31++G** level (Table III). It can thus be concluded that, in both cases, there exists only one complex involving the $HCNH^+$ ion and ethene, that is, **3** or **4**.

Of particular importance is that **1/3** lies, in energy, above the dissociation products **5** whereas **2/4** is situated below **5**. This is easily explained from the calculated structure of the transition structures. As shown in Figure 1, both TS **1/3** and **2/4** consist essentially of a bridged $C_2H_5^+$ cation in interaction with the neutrals HNC and HCN, respectively. Obviously, the large difference between the standard enthalpies of HNC and HCN (201 and 135 kJ mol^{-1} respectively) is reflected to some extent in the energy level of TS **1/3** and **2/4**.

Isomerization **3** ↔ **4** has not been considered by ab initio MO calculations because the critical energy for such a rearrangement involving only a reorientation of the dipole inside an electrostatic complex should be lower than that required for the complete separation of C_2H_4 and $HCNH^+$. In fact, both π-bonded complexes **3** and **4** must transform into more energetic complex structures with a distance between the partners allowing for their required 180° reorientation. These complex structures reside in an energy range below 213 kJ mol^{-1} due to the electrostatic interaction between $HCNH^+$ and the polarizable ethene molecule. As an indication, the stabilization energy provided by a point charge interacting with an ethene molecule at 4 Å distance is found to be 10 kJ mol^{-1}. Thus 213 kJ mol^{-1} is clearly the maximum value for the energy level of an eventual transition structure associated with $\mathbf{3} \rightleftharpoons \mathbf{4}$ and, as long as no products more stable than 213 kJ mol^{-1} are observed, there is no need for a more precise estimation. It should be added that another possible intermediate for $\mathbf{3} \rightleftharpoons \mathbf{4}$ isomerization is the cyclic structure $[CH{=}NH^+\text{-}CH_2CH_2]$ (**10**) whose energy relative to **1** is only 37 kJ mol^{-1} (Figure 1, Table II). This cyclic structure has also been proposed as an intermediate in the fragmentation of $[CH_3C{\equiv}NCH_3]^+$ ions.[14,15]

(b) Isomerization of 1 and 2 via 1,2 H or C_2H_5 Shifts. Reaction routes presented in Scheme II have been investigated only by geometry optimization all the HF/6-31G* level. Relative energies are estimated using MP2(F)/6-311++G** calculations with HF/6-31G* geometries. The results are summarized in Figures

---

(29) DeFrees, D. J.; McLean, A. D. *J. Am. Chem. Soc.* **1985**, *107*, 4350.

(30) Budzikiewicz, H.; Djerassi, C.; Williams, D. H. *Structure Elucidation of Natural Products by Mass Spectrometry*; Holden Day: San Francisco, 1964; Vol. 1, p 22.

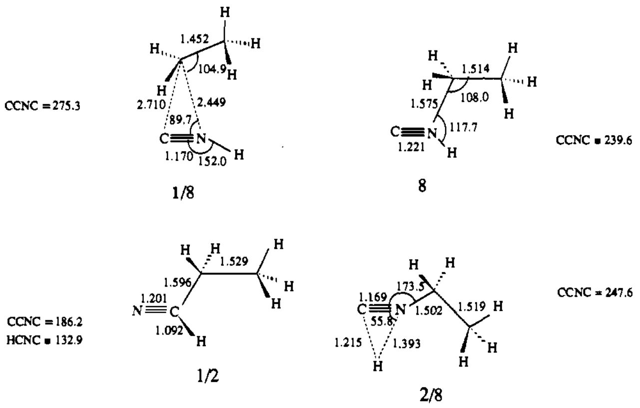

Figure 3. Selected geometrical parameters for structures associated with 1,2-ethyl and 1,2-hydrogen migration from **1** and **2** (HF/6-31G*).

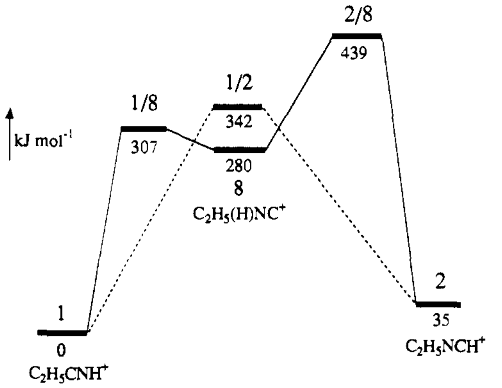

Figure 4. Schematic potential energy profile (in kJ mol^{-1}) showing the isomerization of **1** and **2** (at MP2/6-311++G** + ZPE using HF/6-31G* geometries).

3 and 4 and Table IV. Similar pathways have been explored for lower homologues, essentially to understand the interstellar chemistry of HCNH$^+$,[5-7] CH$_3$CNH$^+$, or CH$_3$NCH$^+$. In this context it is of interest to investigate C$_2$H$_5$CNH$^+$ (**1**) and C$_2$H$_5$NCH$^+$ (**2**).

As in the case of CH$_2$N$^+$ mentioned above, structure **9** does not exist as a local energy minimum but rather a transition structure directly connecting both ions **1** and **2**. The geometry of this TS **1/2** is displayed in Figure 3. Similarly to H$_2$NC$^+$, structure **8** is well characterized as a local minimum and an intermediate between **1** and **2**. The relevant transition structures **1/8** and **2/8** are also displayed in Figure 3.

It is worth noting that the 1,2-ethyl migration requires a smaller activation energy than that of the 1,2-hydrogen migration. A critical energy for the 1,2-ethyl shift of 307 kJ mol^{-1} is estimated (Figure 4). This is similar to the value of ca. 300 kJ mol^{-1} previously computed for the 1,2-methyl shift in the CH$_3$CNH$^+$/CH$_3$NCH$^+$ system.[7] The 1,2-hydrogen shift $2 \rightarrow 8$ requires substantial critical energy (>439 kJ mol^{-1}). Such high critical energies have also been calculated for HCNH$^+$,[4] CH$_3$CNH$^+$,[5-7] and CH$_3$NCH$^+$.[6,7]

Overall, we have found that a direct isomerization $1 \rightarrow 2$, without intermediate, through the TS **1/2** is the most favored process (Figure 4). Nevertheless, the energy barrier remains quite substantial (ca. 342 kJ mol^{-1}) and, more importantly, much larger than those involved in the β-elimination processes described in Figure 1.

The transition structures **1/8** and **1/2** may again be considered as complexes between the C$_2$H$_5$$^+$ cation (in its classical conformation) and neutral HNC or HCN. However, the complexation energies of TS **1/8** and **1/2** are lower than in the case of TS **1/3** and **2/4**. In fact, during bond elongation from **1** or **2** the C$_2$H$_5$$^+$ moiety adopts preferentially a conformation allowing a proton transfer from the methyl group to HNC or HCN, thus leading to **1/3** and **2/4** and β-elimination. Obviously, only the mechanism in Scheme I is appropriate for the description of the chemistry of ions **1** and **2** of low internal energy.

Scheme III

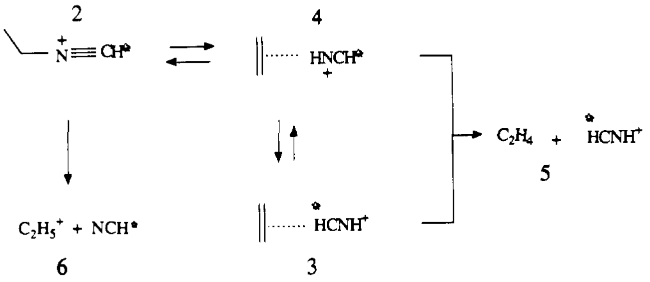

Scheme IV

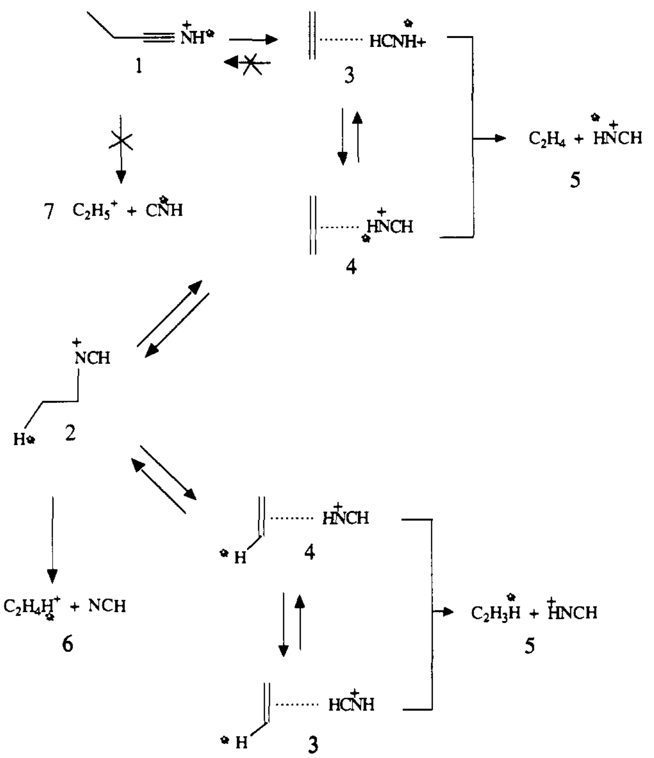

Discussion

The dissociation $2 \rightarrow$ HCNH$^+$ + C$_2$H$_4$ occurs at its thermochemical threshold via specific β-elimination (for at least 96%). This can be explained from calculated energy profile given in Figure 2 and mechanistic details given in Scheme III.

Isomerization $2 \rightleftharpoons 4$ requires less energy than dissociation into fragments **5**; there is thus no energy barrier between **2** and **5** as observed experimentally. The reversibility of steps $2 \rightarrow 4$ and $3 \rightarrow 4$ brings about no mixing of the original proton (labeled with a star in Scheme III) with the hydrogens of the ethyl group, in agreement with the results of deuterium-labeling experiments. Note that our model predicts a complete H-randomization within the ethyl chain, a phenomenon which could be shown by suitable D-labeling.

The competitive fragmentation, i.e., formation of C$_2$H$_5$$^+$ ions, leads to the most stable products **6** without significant loss of identity of the original proton as indicated by the negligible signal at m/z 30 (C$_2$H$_4$D$^+$) in the MIKE spectrum of **2a** (Table I).

The case of protonated ethyl cyanide (**1**) is more complex since the dissociation $1 \rightarrow$ HCNH$^+$ + C$_2$H$_4$ takes place after a rate-determining step which obscurs the specificity of the β-elimination (Figure 2 and Scheme IV).

Before eliminating C$_2$H$_4$, **1** has to isomerize into **3** through the high-energy transition structure **1/3**. This explains the large $T_{0.5}$ value associated with this fragmentation. If some internally excited complexes **3** may lead to **5** via specific β-elimination, some others may as well isomerize into **4** (a lower critical energy process) and further into **2**. These successive isomerizations bring about the mixing of the original proton (labeled with a star in Scheme IV) with four of the five H atoms of the ethyl chain. The results above indicate that only roughly half of the ions **1** react by specific β-elimination.

Moreover, the H-randomization also seems to involve, to some extent, the first H transferred during step $\mathbf{1} \rightarrow \mathbf{3}$. This observation may be accounted for by a partial reversibility of reaction $\mathbf{1} \rightarrow \mathbf{3}$ for metastable ions **1**. Another possibility is the isomerization of **3** or **4** into the cyclic structure $[HC{=}NH{-}CH_2{-}CH_2]^+$ (**10**) followed by C–C ring opening and 1,2 H migration leading to $[CH_3C{=}NCH_3]^+$. It is difficult to evaluate the role of this reversibility as it is only evidenced by low intensity signals (m/z 30 for **1b**, **1c**, and m/z 28 for **1d** and **1e**) and a fortiori to answer with certainty the latter question.

Ions **1** of higher internal energy dissociate into $C_2H_5^+$ ions. It is proposed that, in view of the energy gap between **6** and **7**, only the products **6** can be obtained after the sequence $\mathbf{1} \rightarrow \mathbf{3} \rightarrow \mathbf{4} \rightarrow \mathbf{2} \rightarrow \mathbf{6}$ (Scheme IV). This may explain the similar abundance ratios (m/z 28)/(m/z 29) observed in both MIKE spectra of **1** and **2**. Note that the internal energy content of the metastable ions **1** leading to **6** is sufficient to allow the reversibility of the first step $\mathbf{3} \rightarrow \mathbf{1}$. Thus the C-bonded H atom in $HCNH^+$ is also mixed to some extent with the other five H atoms, and consequently signals corresponding to $C_2H_5^+$ must involve statistically all H of the precursor ion **1** as corroborated by experiment (see, for example, m/z 32 and 31 in **1c**).

Conclusion

The reactivity of low energy both protonated ethyl cyanide (**1**) and ethyl isocyanide (**2**) may be conveniently described by the energy profile in Figure 2; both species interconvert through π-bonded complexes **3** and **4** differing in the mutual orientation of the partners by 180° before their decomposition either into $NCNH^+$ and ethene, or into $C_2H_5^+$ and HCN. The interconversion $\mathbf{3} \rightleftharpoons \mathbf{4}$ requires either the intermediacy of more energetized ion neutral complex structures (less than 224 kJ mol^{-1} though), satisfying the so-called "reorientation criterion",[31] or the addition of the partners into a more stable transient cyclic immonium ion.

The present data also provide new insight into the chemistry of $C_3H_6N^+$ ions from which C_2H_5CN (or C_2H_5NC) may originate via dissociative recombination in interstellar media. It has been shown that isomerization $\mathbf{1} \rightleftharpoons \mathbf{2}$ requires ca. 250 kJ mol^{-1} (Figure 2). Consequently, ion **1** whose internal energy is lower than 250 kJ mol^{-1} will produce only C_2H_5CN molecules by the reaction $\mathbf{1} + e \rightarrow C_2H_5CN + H^\bullet$, while the more energetic ions **1** are likely to produce a mixture of C_2H_5CN and C_2H_5NC. Hence, whether C_2H_5NC exists in interstellar clouds along with C_2H_5CN strongly depends on the internal energy content of **1** and thereby on its origin whose knowledge is crucial.

Further work is in progress on other $C_3H_6N^+$ isomers such as $[CH_2{=}CH{-}CH{=}NH_2]^+$ and higher homologues in order to get a deeper understanding of the complex chemistry of these ionic species.

Acknowledgment. M.T.N. is a Research Associate of the National Fond for Scientific Research (NFWO, Belgium). We thank the Ecole Polytechnique for financial support and KU Leuven for a grant of computer time.

---

(31) (a) Bowen, R. D. *Acc. Chem. Res.* **1991**, *24*, 364. (b) Morton, T. H. *Org. Mass Spectrom.* **1992**, *27*, 353. (c) Longevialle, P. *Mass Spectrom. Rev.* **1992**, *11*, 157.

Cation–Framework Interaction in Alkali-Cation-Exchanged Zeolites: An XPS Study

M. Huang, A. Adnot, and S. Kaliaguine*

Contribution from the Département de Génie Chimique et CERPIC, Université Laval, Québec, Canada. *Received May 18, 1992*

Abstract: A series of alkali-cation-exchanged and also some proton-exchanged zeolites have been investigated using XPS. The larger the electropositivity of the countercation is, the lower the framework element (Si_{2p}, Al_{2p}, and O_{1s}) binding energies are. However, the extent of these changes depends strongly on the Si/Al ratio of zeolites. On the basis of the changes in N_{1s} binding energy and previous infrared results for the chemisorbed pyrrole probe molecule, evidence is offered to support the hypothesis that the cation–framework interaction in zeolites is limited to a short-range scope. On the basis of this kind of short-range interaction, a model for pyrrole chemisorption is suggested and the charges on N, Si, and Al are then calculated using the Sanderson electronegativity equalization method. The calculated charges correlate well with the observed binding energies of the corresponding elements. The results further suggest that the probe molecules containing N atoms are sensitive indicators of charge transfer in XPS experiments. The Si_{2p} binding energy level is not a good internal reference binding energy in XPS spectra for zeolites possessing a low Si/Al ratio.

Introduction

The bonding chemistry in zeolites has been discussed by Mortier and Schoonheydt.[1] Using Gutmann's interatomic interaction rules and the Sanderson electronegativity equalization principle, they proposed an electron donor–acceptor interaction between the extraframework cations and the framework atoms. The same topic was also investigated by Barr,[2] on the basis of a series of XPS studies.[2-4] A group shift concept is suggested to explain why the binding energies of all zeolite elements shift in the same direction with a change in the Si/Al ratio. According to this concept, the two groups involved in zeolites are silica (SiO_2) and metal aluminate. The formation of zeolites from these two groups will result in an increase in binding energies of all zeolite elements with an

---

* To whom correspondence should be addressed.

(1) Mortier, W. J.; Schoonheydt, R. A. *Prog. Solid State Chem.* **1985**, *16*, 1.

(2) Barr, T. L. *Zeolites* **1990**, *10*, 760.

(3) Barr, T. L. In *Practical Surface Analysis*; Briggs, D., Seah, M. P., Eds.; John Wiley: Chichester, U.K., 1983; Chapter 8.

(4) Barr, T. L.; Lishka, M. A. *J. Am. Chem. Soc.* **1986**, *108*, 3178.

0002-7863/92/1514-10005$03.00/0